Lipid-Encapsulated mRNAs Encoding Complex Fusion Proteins Potentiate Antitumor Immune Responses

Casey W. Shuptrine[1], Yuhui Chen[1], Jayalakshmi Miriyala[1], Karen Lenz[1], Danielle Moffett[1], Thuy-Ai Nguyen[1], Jenn Michaux[1], Kristen Campbell[1], Connor Smith[1], Marc Morra[1], Yisel Rivera-Molina[1], Noah Murr[1], Sarah Cooper[1], Ashlyn McGuire[1], Vishruti Makani[1], Nathan Oien[1], Jeffery T. Zugates[1], Suresh de Silva[1], Taylor H. Schreiber[1], Seymour de Picciotto[2], and George Fromm[1]

ABSTRACT

Lipid nanoparticle (LNP)–encapsulated mRNA has been used for *in vivo* production of several secreted protein classes, such as IgG, and has enabled the development of personalized vaccines in oncology. Establishing the feasibility of delivering complex multispecific modalities that require higher-order structures important for their function could help expand the use of mRNA/LNP biologic formulations. Here, we evaluated whether *in vivo* administration of mRNA/LNP formulations of SIRPα-Fc-CD40L and TIGIT-Fc-LIGHT could achieve oligomerization and extend exposure, on-target activity, and antitumor responses comparable with that of the corresponding recombinant fusion proteins. Intravenous infusion of the formulated LNP-encapsulated mRNAs led to rapid and sustained production of functional hexameric proteins *in vivo*, which increased the overall exposure relative to the recombinant protein controls by ∼28 to 140 fold over 96 hours. High concentrations of the mRNA-encoded proteins were also observed in secondary lymphoid organs and within implanted tumors, with protein concentrations in tumors up to 134-fold greater than with the recombinant protein controls 24 hours after treatment. In addition, SIRPα-Fc-CD40L and TIGIT-Fc-LIGHT mRNAs induced a greater increase in antigen-specific $CD8^+$ T cells in the tumors. These mRNA/LNP formulations were well tolerated and led to a rapid increase in serum and intratumoral IL2, delayed tumor growth, extended survival, and outperformed the activities of benchmark mAb controls. Furthermore, the mRNA/LNPs demonstrated improved efficacy in combination with anti-PD-L1 relative to the recombinant fusion proteins. These data support the delivery of complex oligomeric biologics as mRNA/LNP formulations, where high therapeutic expression and exposure could translate into improved patient outcomes.

Significance: Lipid nanoparticle–encapsulated mRNA can efficiently encode complex fusion proteins encompassing immune checkpoint blockers and costimulators that functionally oligomerize *in vivo* with extended pharmacokinetics and durable exposure to induce potent antitumor immunity.

Introduction

At the core of the successful global response to the SARS-CoV-2 pandemic lies decades of research dedicated to the synthesis of mRNAs incorporating unique sequence elements and modifications. These modifications enhance their stability and translation efficiency. To enable their effective delivery, lipid nanoparticles (LNP) have been developed to encapsulate the mRNA cargo, providing protection and facilitating transport into the cytosol of target cells (1, 2). mRNA/LNP technology has been applied to a wide variety of protein formats, including the expression of a full-length neutralizing antibody to chikungunya virus (3–6). Application of mRNA/LNP technology to antibodies requires the separate expression and pairing of both immunoglobulin heavy and light chains into the appropriate quaternary structure for secretion, stability, and function *in vivo*. Other advances have enabled the development of personalized vaccines in oncology, including mRNA-4157, wherein patient-specific tumor antigens are rapidly identified and assembled as concatemers into a continuous mRNA capable of stimulating antitumor immune responses. In patients with high-risk melanoma, mRNA-4157 in combination with pembrolizumab, resulted in recurrence free survival at 18 months in 78.6% of patients, compared with 62.2% of patients with pembrolizumab alone (7, 8). Current efforts aimed at enhancing the systemic safety of mRNA/LNP formulations, and reducing immunogenicity risks following repeated administration, are beginning to show promise in clinical studies, and may open the door for broader proliferation of mRNA/LNP formulations of biologics as an economical alternative to mass-produced recombinant proteins (9). Thus, establishing feasibility for the expression and assembly of complex biologics when delivered as mRNA/LNP formulations, and comparing the biologic properties of *in vivo* expressed biologics to bolus-injected recombinant proteins, are important goals.

SIRPα-Fc-CD40L and TIGIT-Fc-LIGHT are two such biologics that have been developed as recombinant Fc-fusion proteins in humans and nonhuman primates, respectively (**Fig. 1A**; refs. 10–12). Each of these recombinant proteins are expressed from single continuous open reading frames (ORF) by CHO cells. Following the expression of a protein monomer, covalent dimers form through interchain disulfide bonds in the Fc region of the protein. Dimers then assemble first into tetramers and ultimately hexamers due to noncovalent trimerization by the TNF ligand domains (**Fig. 1B** and **C**; refs. 10, 11, 13, 14). This oligomerization

[1]Shattuck Labs Inc., Austin, Texas. [2]Moderna, Inc., Cambridge, Massachusetts.

Corresponding Author: George Fromm, 21 Alexandria Way, Suite 200, Durham, NC 27709. E-mail: gfromm@shattucklabs.com

Cancer Res 2024;84:1550–9

doi: 10.1158/0008-5472.CAN-23-2875

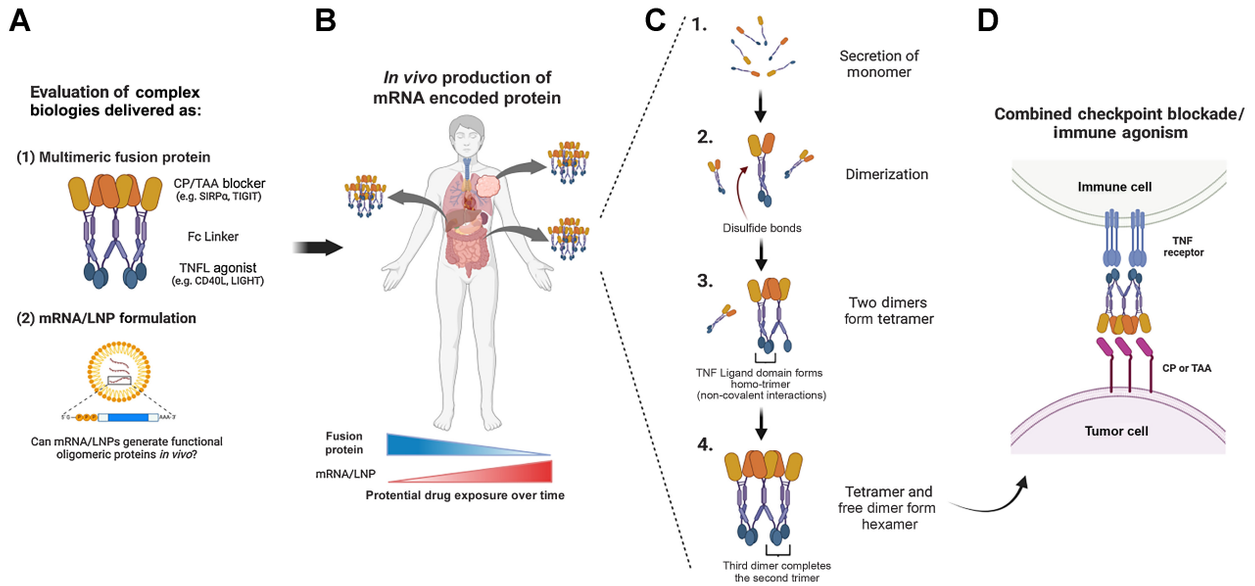

Figure 1.

Proof of concept: Can mRNA/LNP formulations encode active multimeric biologics *in vivo*? **A**, Complex, hexameric bifunctional therapies that simultaneously block an immune checkpoint (CP) or tumor associated antigen (TAA) and agonize TNF receptor/ligand (TNFR / TNFL) pathways have been successfully manufactured as fusion protein biologics and are under clinical investigation in multiple oncology trials. **B,** The mRNA/LNP generation of similar multimeric therapeutics could influence certain attributes of pharmacokinetics and pharmacodynamics, including the *in vivo* production from multiple tissue compartments over an extended time course as compared with the fusion protein exposure kinetics. **C,** Fc-linked hexameric fusion proteins produced from mammalian production cell lines are secreted as monomers that go through a stepwise process of disulfide mediated dimerization, followed by tetramer and then hexamer formation through noncovalent interactions between neighboring TNF-ligand domains. **D,** The resulting hexameric fusion protein uniquely activates TNF-receptors, which require trimerization for signaling. (Created with BioRender.com.)

is crucial for the activity of TNF-ligands and their cognate TNF receptors (like CD40, 4–1BB, OX40, and others), which require trimerization in the cell membrane to effectively signal and induce immune cell agonism (**Fig. 1D**; refs. 14–16).

The goals of this study were to determine the efficiency of expression of *SIRPα-Fc-CD40L* and *TIGIT-Fc-LIGHT* as mRNA/LNP formulations, assess whether the mRNA-encoded proteins attained functional hexameric structures *in vivo*, and to compare the biological activity of the mRNA/LNP expressed constructs to the corresponding recombinant fusion protein reference material (**Fig. 1B**; FP ref.). We found that intravenous infusion of mRNA/LNPs was well tolerated, and concentrations of the mRNA-encoded protein exceeded that of the FP ref. protein within 2 hours of delivery in serum and other tissues. The primary structure of the mRNA-encoded protein in the serum of treated animals *in vivo* was confirmed to be a hexamer, as the high serum concentrations facilitated purification and SEC analysis of the oligomer composition. To further confirm the potency of hexameric *SIRPα-Fc-CD40L* and *TIGIT-Fc-LIGHT* as lipid encapsulated mRNAs, the pharmacodynamic and antitumor activity of these formulations was compared with the well characterized recombinant protein equivalents using a large established CT26 colorectal carcinoma tumor model. In total, these studies confirmed that lipid-encapsulated mRNA encoding *SIRPα-Fc-CD40L* and *TIGIT-Fc-LIGHT* dramatically extended the *in vivo* exposure of predominantly hexameric fusion proteins, with improved pharmacodynamic and antitumor effects when compared head-to-head against the corresponding recombinant protein. Taken together, these results support the evaluation of complex secreted biologics by mRNA/LNP delivery.

Materials and Methods

Material generation and characterization

The generation of FP ref. material was accomplished as previously described, through transient production in CHO cells followed by affinity capture of the mouse constructs using protein A and human constructs using FcXL, followed by elution and buffer exchange (10, 11). mRNA constructs were synthesized by *in vitro* transcription (IVT) followed by DNase digestion. A plasmid encoding the T7 RNA polymerase promoter followed by 5′-untranslated region (UTR), open reading frame (ORF), 3′-UTR, and polyA tail was overexpressed in *E. coli*, linearized, and purified to homogeneity. The mRNA was synthesized by using a modified T7 RNA polymerase IVT, where uridine triphosphate was substituted completely with N1-methyl-pseudouridine triphosphate. Cap 1 was utilized to improve translation efficiency (17). After the transcription reaction, mRNAs were purified, buffer exchanged into sodium citrate, and stored at −20°C until use. Formulation of mRNA were performed as described previously (18). Analytical characterization assays included particle size and polydispersity, encapsulation, and endotoxin content, which had to meet predefined specifications before the material was deemed acceptable for *in vivo* study. The mRNA was encapsulated in a lipid nanoparticle through a modified ethanol-drop nanoprecipitation process described previously (18). Briefly, ionizable, structural, helper, and PEG lipids were mixed with mRNA in acetate buffer, pH 5.0, at a ratio of 3:1 (lipids: mRNA). The mixture was neutralized with Tris-Cl, pH 7.5, sucrose was added as a cryoprotectant, and the final solution was sterile filtered. Vials were filled with formulated LNP and stored frozen at −70°C until further use. The final drug product underwent

analytical characterization, which included the determination of particle size and polydispersity, encapsulation, mRNA purity, and endotoxin. Final particle size and encapsulation were <100 nm and >80%, respectively, with endotoxin below 10 EU/mL. Both FP ref. material and protein encoded by mRNA contain a wild-type mouse IgG_1 central domain.

In vitro functional activity

HEK293 transfection

One micrograms of naked mRNA with Lipo2000 was used to transfect HEK293T cells (RRID:CVCL_0063). After 24 or 48 hours, cell culture supernatant was collected, and mouse and human mRNA-encoded proteins were purified as described above. SDS-PAGE was used to characterize the purified FP using antibodies targeting mouse and human SIRPα, CD40L, TIGIT, LIGHT, or Fc (R&D Systems and The Jackson Laboratory). mRNA-encoded FP were quantitated using mesoscale discovery (MSD) as described using the corresponding recombinant FP control as a standard (12).

MSD potency

Dual target binding MSD assays were developed for each construct to ensure full-length protein was capable of engaging its intended targets at the same time, as described previously (10, 11). Here, FP ref. and mRNA-encoded proteins were assessed using capture/detect reagents to mouse and human CD47/CD40 or PVR/HVEM.

Cell-based potency assays

CHOK1-CD40/NFκB-luciferase cells were generated previously (10) and used to assess luciferase dose responses of FP ref. and mRNA-encoded material. Macrophage/tumor phagocytosis assays were performed as described previously (10). RAW264.7-Lucia-ISG-reporter cells (InvivoGen, RRID:CVCL_X596) were used according to manufacturer recommendations to assess CD40 activation of a type I IFN stimulatory reporter in the presence of mouse SIRPα-Fc-CD40L FP ref. or the mRNA-encoded material. PathHunter U2OS/LTβR/NIK/NFκB reporter cells (DiscoverX) were used according to manufacturer recommendations to assess the activity of TIGIT-Fc-LIGHT FP ref. and mRNA material. LTβR+ A375 (RRID:CVCL_0132) or CT26 (RRID:CVCL_7254) tumor cell lines were cultured with test agents for 3 hours before reverse transcribing cDNA to assess the expression of *ACTB/Actb, CXCL8, CCL2/Ccl2*, and *Cxcl5* using qPCR with SYBR Green reagents, validated primer sequences from Origene, and the Bio-Rad CFX96 Touch real-time PCR detection system. Fold change in gene expression was determined using the ΔΔCt method relative to the housekeeping gene *ACTB* (11).

Reporter cell lines were obtained from the indicated vendors. Parental cell lines were purchased from ATCC. Cells in active culture were passaged two to three times per week, kept in culture for a maximum of 2 months, and tested monthly using the Venor GeM Mycoplasma Detection Kit (Sigma). All transfected cell lines were tested an additional two times post transfection, separated by at least 2 weeks, and confirmed to remain negative for mycoplasma.

In vivo PK, PD, and antitumor activity

Pharmacokinetics

BALB/c (8- to 12-week-old female; The Jackson Laboratory, RRID:MGI:2161072) mice were given a single intravenous tail vein injection of vehicle (PBS), mRNA/LNP constructs (0.5 mg/kg or 12.5 μg in total), or FP reference material (8 mg/kg or 200 μg in total); 3 mice per group per time point. Tissues and serum were isolated and cell lysates were prepared at the indicated timepoints to determine FP concentrations using a MSD-dual binding assay, and normalized as picogram or nanogram per gram of starting tissue. For SEC, serum samples were diluted with PBS and loaded onto an AKTA Start protein purification system at a flow rate of 0.11 mL/min, using a 1 mL HiTrap column and Amsphere A3 protein A resin. Eluted material was assessed by SEC using a Thermo Fisher Scientific Vanquish system with a Bio SEC-5 (Agilent, 500Å, 5 μm, 7.8 ID × 300 m).

Pharmacodynamics

Serum chemistries were evaluated by the Pathology Service Core and Animal Clinical Laboratory Medicine Core at the University of North Carolina at Chapel Hill, using the Vet Axcel Chemistry Analyzer (Alfa Wassermann). Serum and tumor lysate cytokines were assessed using a custom MSD multiplex plate according to manufacturer instructions. Resulting data were plotted in heatmap format depicting row min/max values across samples. Hierarchical clustering (1 − Spearman correlation) was used to demonstrate group and cytokine associations.

Tumor efficacy

BALB/c mice (8–12 weeks old) were subcutaneously implanted with 5×10^5 CT26 tumor cells into the hind right flank. When tumors were approximately 90 mm^3 (8 days after inoculation on average) mice were randomized across treatment groups and treatment was initiated (indicating day 0). Tumor-bearing mice were treated via intraperitoneal injections with recombinant fusion proteins (200 μg per dose) and antibodies 100 μg per dose for anti-CD47 (clone MIAP410 BioXCell, RRID:AB_2687806) and anti-TIGIT (clone 1G9 BioXCell, RRID:AB_2687797) or 200 μg per dose for anti-PDL1 (clone 10F.9G2, RRID:AB_10949073) or via intravenous injection for the mRNA/LNP constructs (0.5 mg/kg per dose) on days 0, 3, 7, 10, 14, and 17 of a 30-day time course. The antitumor efficacy benchmark for these fusion protein constructs and antibodies has previously been described using intraperitoneal administration, and we and others have shown that intraperitoneal and intravenous administration in mice results in similar drug exposure levels (Supplementary Fig. S1A; refs. 10, 11, 19). Tumor volume (mm^3) and overall survival were assessed throughout the time course. Animals were humanely euthanized when total tumor volume reached >1,800 mm^3 or there were signs of significant tumor ulceration. Individual animal tumor growth curves, the average time in which each treatment group reached full tumor burden, the number of mice that rejected the primary tumor (tumor volume ≤0.5 mm^3), and overall survival were assessed over a 30-day time course. On day 8 of the study, a group of treated animals was euthanized, and necropsy was performed to collect serum and tumor tissue for PK, cytokine, and flow cytometry analysis.

Flow cytometry

Tumor tissue was dissociated using an enzymatic tumor dissociation kit (Miltenyi Biotec), and the resulting cells were exposed to a viability dye and then Fc receptors were blocked (both BioLegend). Cell staining was performed for 30 minutes at 4°C in the dark. For Foxp3 staining, the Foxp3 Fix/Perm Buffer Kit (BioLegend) was used according to manufacturer instructions. After antibody incubations, cells were washed 2× in 500 μL FACS buffer (1× DPBS, 1%BSA, 2 mmol/L EDTA, and 0.02% NaN_3), and then analyzed on the BD LSR Fortessa Cell Analyzer.

Experimental animal guidelines

All experimental mice used were female inbreed BALB/c co-housed during the course of an experiment (The Jackson Laboratory). All murine animal studies have been conducted in accordance with, and with the approval of an Institutional Animal Care and Use Committee (IACUC); and reviewed and approved by a licensed veterinarian.

Statistical analysis

Unless noted otherwise, values plotted represent the mean and error is SEM. Statistical significance (*P* value) was determined using one-way ANOVA with multiple comparisons. Significant *P* values are *, $P < 0.05$; **, $P < 0.01$; ***, $P < 0.001$; ****, $P < 0.0001$. Mantel–Cox statistical tests were used to determine the significance between the survival curves.

Data availability

Data were generated by the authors and included in the article. All raw data are available upon request from the corresponding author.

Results

mRNA encoding mouse and human *SIRPα-Fc-CD40L* and *TIGIT-Fc-LIGHT* were transiently transfected into HEK293T cells and after 24 or 48 hours, supernatant was collected and affinity purified. The resulting protein was assessed using SDS-PAGE and were detected with three separate domain-specific antibodies. All three detection methods indicated full length proteins migrating at the expected monomeric molecular weights of 88.1 kDa for SIRPα-Fc-CD40L and 59.3 kDa for TIGIT-Fc-LIGHT (**Fig. 2A** and **B**; Supplementary Figs. S1B and S1C; refs. 10, 11). Secreted protein concentrations were evaluated using a dual-binding MSD method, normalized on a per-cell-basis and found to reach 7.76 pg/cell at 24 hours and 27.4 pg/cell at 48 hours for human *SIRPα-Fc-CD40L*, and 4.46 pg/cell at 24 hours and 8.98 pg/cell at 48 hours for human *TIGIT-Fc-LIGHT*, which are on par with the productivity achieved from commercial CHO and 293 based biomanufacturing processes (**Fig. 2C** and **D**; ref. 20). Parallel studies using the mouse-equivalent mRNA constructs showed similar results (Supplementary Figs. S1D and S1E).

The potency of the mRNA-encoded proteins was assessed using (i) dual-target MSD potency, (ii) cell-based CD40/NFκB-luciferase reporter, and (iii) *in vitro* species-specific macrophage phagocytosis assays for *SIRPα-Fc-CD40L* (**Fig. 2C**). In addition, a RAW264.7/ISG (IFN stimulatory gene) reporter cell line was used to inform on the activation of interferon response pathways downstream of CD40 ligation (Supplementary Fig. S1D, parts 1–4). Human mRNA-encoded *TIGIT-Fc-LIGHT* was assessed using (i) dual-target MSD potency, (ii) cell-based U2OS/LTβR/NFκB/Nik-luciferase reporter, and (iii) through the activation of *CCL2* and *CXCL8* expression in LTβR+ A375 tumor cells (**Fig. 2D**). Mouse TIGIT-Fc-LIGHT activity was assessed using a (i) dual-target MSD potency, and (ii) through the activation of *Ccl2* and *Cxcl5* expression in LTβR+ CT26 tumor cells (**Fig. 2D**). The recombinant fusion protein material (FP ref.) was used as a reference standard to calculate the concentration of the mRNA supernatants. In all cases, the mRNA-encoded fusion proteins demonstrated equivalent potency to that of the FP ref. material. Taken together, the *in vitro* results suggested that both *SIRPα-Fc-CD40L* and *TIGIT-Fc-LIGHT* were efficiently produced from mRNA/LNPs and assembled into functional higher-order quaternary structures capable of agonizing trimeric TNF receptors in various cell-based potency assays.

To determine whether expression and bioactivity was achievable *in vivo*, BALB/c mice were given a single tail vein injection of 0.5 mg/kg (12.5 μg) of the LNP formulated mRNA or 8 mg/kg (200 μg) of the FP ref. After 0.5, 1, 2, 6, 24, 48, 72, and 96 hours, serum, liver, spleen, and iLN were isolated from treated animals for the analysis of serum chemistries and cytokines, and serum and tissue quantification of mRNA encoded protein (**Fig. 3A**). All test articles were well tolerated and no significant elevations of ALT, AST, LDH, creatinine, or total bilirubin were observed over that of the vehicle treated group (Supplementary Fig. S1F). Dual MSD PK assays (capture with antimouse CD40L and detect with antimouse SIRPα or capture with antimouse LIGHT and detect with antimouse TIGIT) were used to assess serum concentrations of the fusion proteins delivered as recombinant protein or mRNA/LNP formulations. As expected, the serum concentration for bolus injected recombinant SIRPα-Fc-CD40L and TIGIT-Fc-LIGHT was highest at the first post-dose timepoint (0.5 hours) and decreased rapidly thereafter (**Fig. 3B**). The targets for SIRPα-Fc-CD40L (CD47 and CD40) are more abundant than the targets for TIGIT-Fc-LIGHT (PVR, HVEM, LTβR), and accordingly both the C_{max} (maximum concentration) and AUC were higher for TIGIT-Fc-LIGHT as compared with SIRPα-Fc-CD40L (**Fig. 3B**; refs. 10–12). Remarkably, serum *SIRPα-Fc-CD40L* and *TIGIT-Fc-LIGHT* were detectable at the earliest timepoint in both mRNA/LNP-treated groups, and the concentration of protein remained consistently high across the entire time course. Further, the concentration of mRNA/LNP expressed proteins remained higher than the C_{max} in the recombinant protein treated groups through 48 hours for *SIRPα-Fc-CD40L* and through the entire 96-hour time course for *TIGIT-Fc-LIGHT*. The overall protein C_{max} from *SIRPα-Fc-CD40L* mRNA treatment was 1.8-fold higher than the FP ref. and was not achieved until 12 hours post-dose, compared with 0.5 hours for the FP ref. control. The AUC from *SIRPα-Fc-CD40L* mRNA was 140-fold greater than that achieved with the FP ref. (**Fig. 3B**). Similar kinetics were observed with *TIGIT-Fc-LIGHT* mRNA, with a C_{max} 6.1-fold higher, and an AUC 28.7-fold greater than that seen with the FP ref. material. The maximum serum concentration for *TIGIT-Fc-LIGHT* was not reached until 32 hours post-dose (t_{max}) compared with 0.5 hours for the FP ref. In addition to achieving elevated concentrations in the serum, both mRNA/LNP formulations also translated to higher concentrations with more sustained exposures in the liver, spleen, and inguinal lymph nodes (**Fig. 3C**).

To assess the oligomeric structure, we took advantage of the high serum concentrations of mRNA-encoded fusion proteins, which facilitated affinity purification of SIRPα-Fc-CD40L directly from the serum of treated animals, followed by size exclusion chromatography (SEC). When the absorbance spectrum from the mRNA/LNP serum sample was overlayed with a known and well-characterized human SIRPα-Fc-CD40L reference standard, the serum isolated mRNA-encoded material was found to closely share the oligomeric profile and existed primarily as a hexamer (**Fig. 3D**).

The administration of both *SIRPα-Fc-CD40L* and *TIGIT-Fc-LIGHT* mRNA/LNPs led to significantly elevated serum concentrations of IL2, which persisted for 48 to 96 hours following a single dose (**Fig. 3E**). With the FP reference material, we have previously observed transient increases in IL2 and other innate and adaptive immune cytokines, including IL2, MCP5, IP10, and MIP1β, and observed similar results here (**Fig. 3F**; refs. 10, 11).

We next evaluated the pharmacodynamic and antitumor responses in mice bearing CT26 colorectal tumors. Some mice were euthanized 24 hours post-dose and tumor tissue was dissociated and fusion

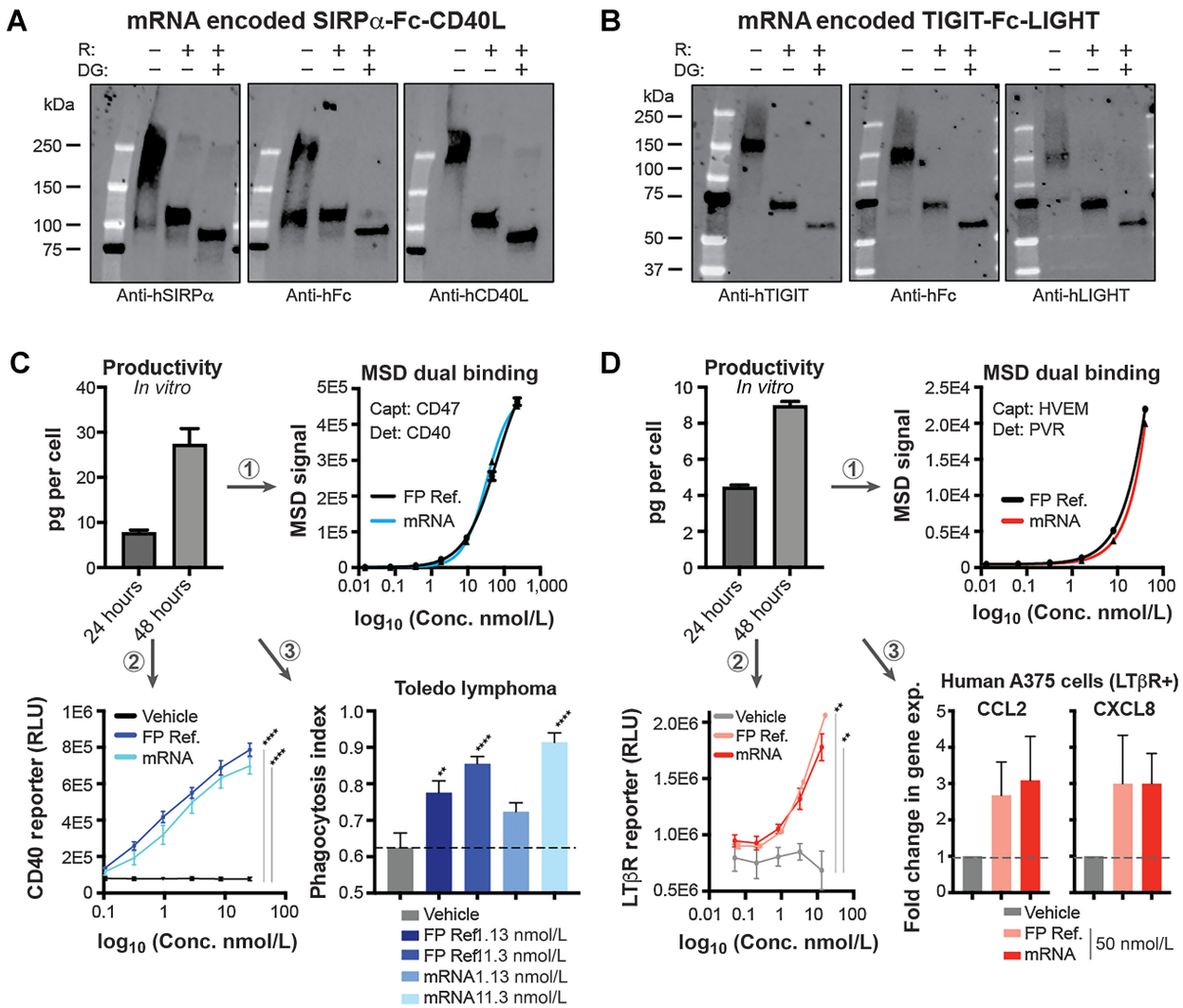

Figure 2.

mRNA constructs encoded functional hexameric bifunctional therapeutic fusion proteins. **A** and **B,** mRNA-encoded human SIRPα-Fc-CD40L (**A**) or TIGIT-Fc-LIGHT (**B**) was transfected into HEK293T cells and after 48 hours, the resulting protein was affinity purified using FcXL resin. The purified protein migrated as expected in SDS-PAGE under nonreduced, BME-reduced (R) and deglycosylated (DG) conditions, and was detected by three separate domain-specific antibodies. **C** and **D,** Per cell production of mRNA generated protein was quantitated using a dual MSD PK assay and two separate VHH reagents developed to be hexameric-fusion protein specific for capture and detection. **C,** The mRNA generated supernatant concentrations were matched to that of fusion protein reference material (FP Ref.) and both the FP ref. and mRNA-generated protein (mRNA) were assessed head-to-head for SIRPα-Fc-CD40L in (**1**) a dual MSD potency assay, (**2**) CD40 cell-based NFκB activity assay, and (**3**) an *in vitro* macrophage/tumor phagocytosis assay. **D,** Human *TIGIT-Fc-LIGHT* was also encoded by mRNA and characterized by Western blot analysis and a dual PK MSD assay. The resulting mRNA-generated protein concentrations were normalized to a FP ref. and assessed head-to-head in (**1**) a dual MSD potency assay, (**2**) a U2OS/NFκB/NIK/LTβR+ cell-based reporter assay, and (**3**) by qPCR assessing the expression of *CCL2* and *CXCL8* in the LTβR+ human tumor cell line A375. **, $P < 0.01$; ****, $P < 0.0001$.

protein concentrations were assessed. In the *SIRPα-Fc-CD40L* group, 122-fold more protein was detected in the tumors of mRNA/LNP treated animals compared with that of the FP ref. (220 pg/g of tissue vs. 1.8 pg/g). In the *TIGIT-Fc-LIGHT* group, 134.8-fold more protein was detected in the tumors of mRNA/LNP treated animals compared with that of the FP ref. (13.48 ng/g of tissue vs. 0.1 ng/g; **Fig. 4A**). The increased serum and tissue exposures (including in the tumor) mediated by the mRNA/LNP delivery of *SIRPα-Fc-CD40L* and *TIGIT-Fc-LIGHT*, resulted in higher levels of serum and intratumor expressed cytokines and chemokines (**Fig. 4B**). In both the serum and tumor, unbiased hierarchical clustering associated the SIRPα-Fc-CD40L and TIGIT-Fc-LIGHT treatment groups (both mRNA/LNP and FP ref.) in proximity, suggesting that both therapeutic delivery methods achieved similar on-target pharmacodynamic activity. In the tumor, the mRNA/LNP and FP ref. groups clustered a single branch apart and appeared to differ by the overall magnitude of response, which was greater and broader in the mRNA/LNP groups than what was observed with the FP reference material. Here, increased tumor levels of IL2, IFNγ, IL12p70, MDC, TNFα, MIP1α, MIP1β, MIP3α, and MCP1, were observed in all mRNA/LNP and FP ref. treatment groups

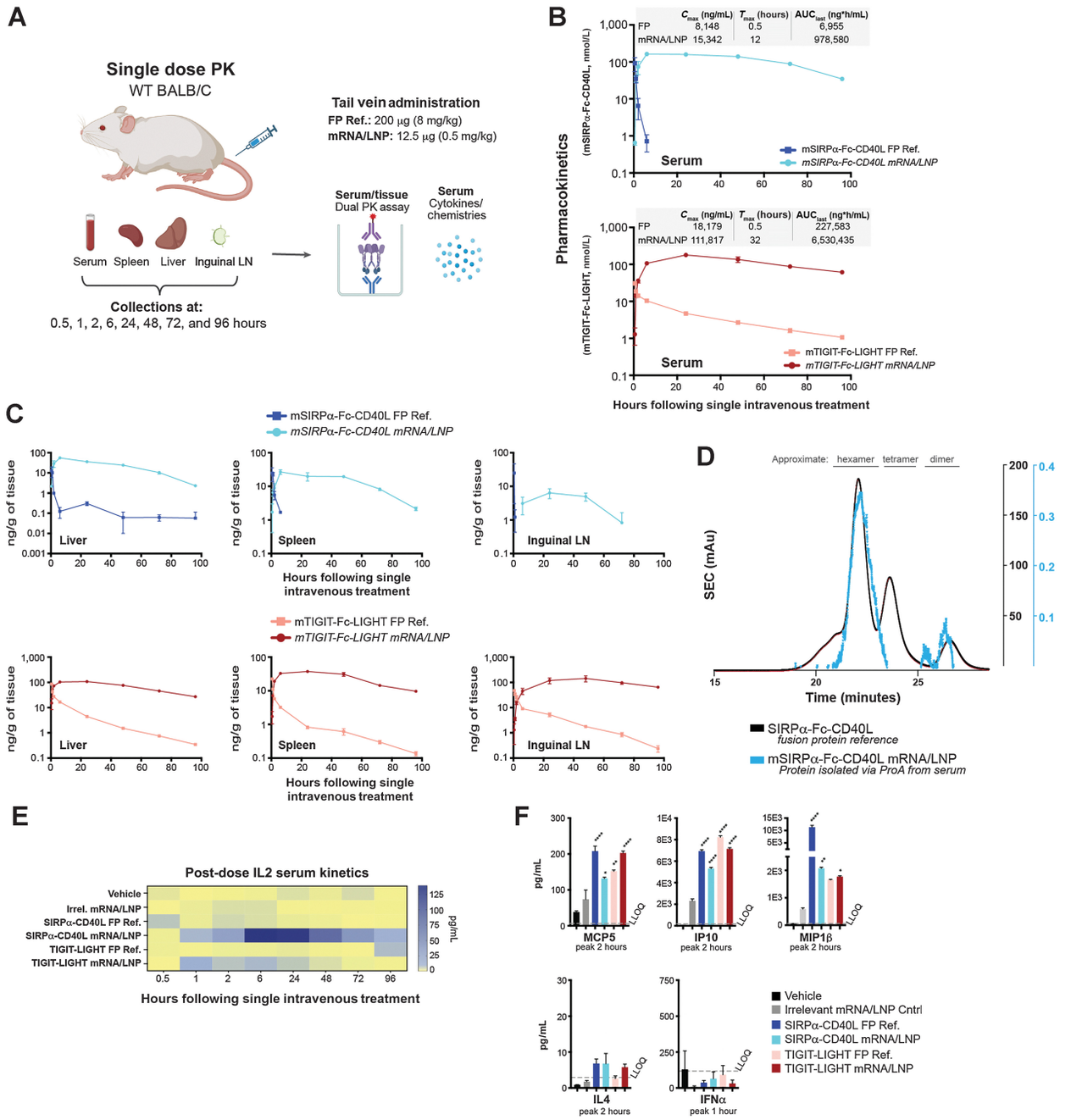

Figure 3.

mRNA-encoded fusion proteins were generated *in vivo* as hexameric proteins and demonstrated extended serum and tissue exposure kinetics. **A,** Mice were given a single dose through tail vein of 200 μg of the FP ref., 12.5 μg of the corresponding mRNA/LNP formulation, or vehicle. **B** and **C,** After 0.5, 1, 2, 6, 24, 48, 72, and 96 hours, serum (**B**) and liver, spleen, and iLNs (**C**) were collected from each animal ($n = 3$ per group, per time point), and PK was assessed using MSD assay formats that captured one end of the fusion protein and detected the other. **D,** Serum was collected from mRNA/LNP-treated mice, pooled, and purified using a single-step ProA capture and elute method. The resulting protein was analyzed using SEC alongside of an existing human SIRPα-Fc-CD40L FP ref. control. **E,** Serum cytokines were assessed in nontumor bearing mice over the entire time course, including the kinetic increase in IL2 over a 96-hour period. **F,** Other cytokines were more transiently increased, usually within 1 to 2 hours of the treatment. *, $P < 0.05$; **, $P < 0.01$; ****, $P < 0.0001$. (**A,** Created with BioRender.com.)

compared with vehicle or benchmark checkpoint inhibitor antibody reference controls (anti-CD47 or anti-TIGIT; **Fig. 4B**). These proinflammatory cytokines have been associated with the activation of myeloid cells through both CD40 and LTβR (11, 21). However, interesting construct-dependent differences in the magnitude of cytokine expression were seen in the serum and tumors of treated animals, including for MIP1β, MCP1, MIP2, and MDC (**Fig. 3B, E,** and **F**; Supplementary Fig. S1G; refs. 10–12).

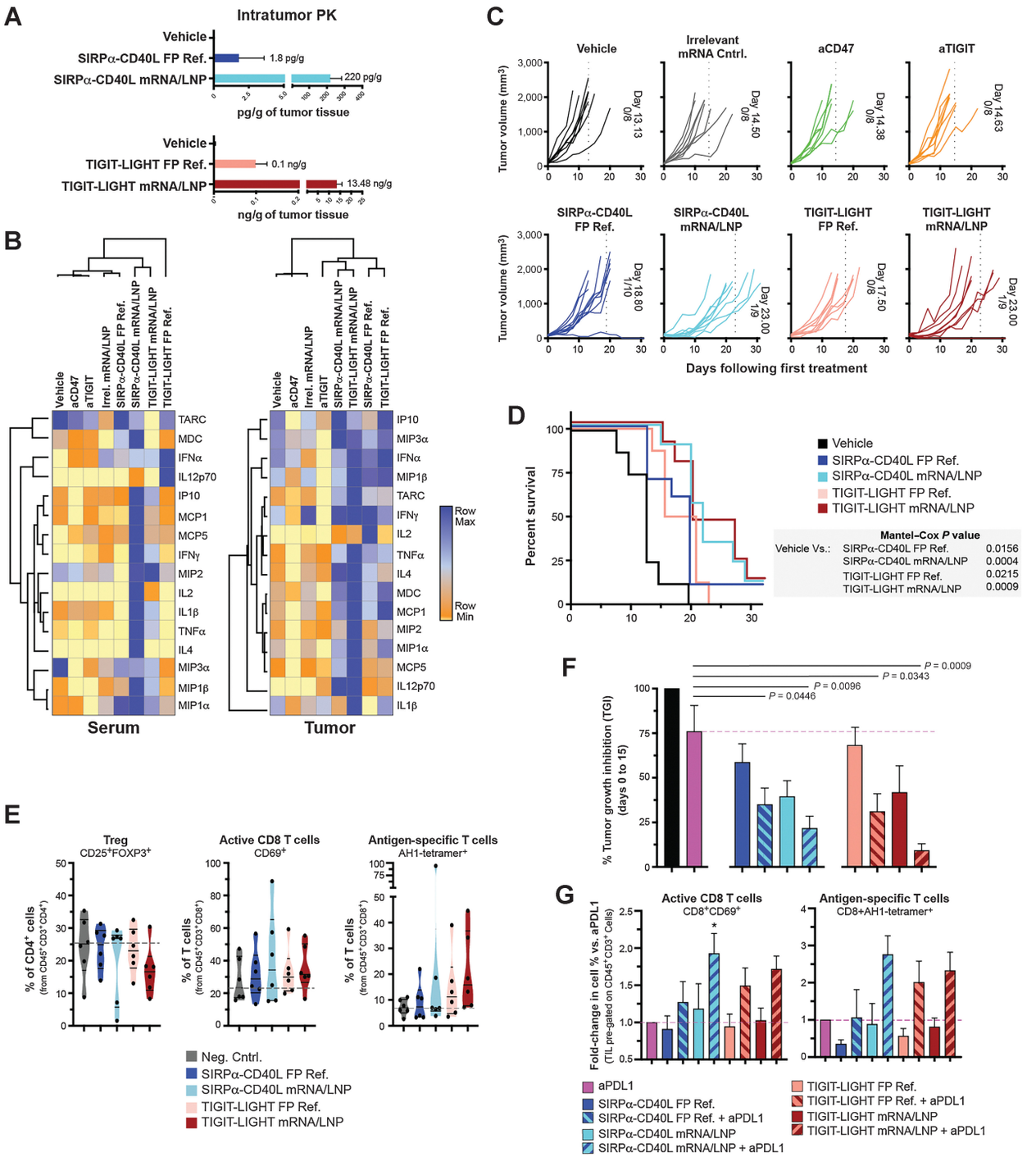

Figure 4.

mRNA-encoded fusion proteins detected in the tumor and induced on-target PD activity, antitumor response, and extended survival. A CT26 tumor study was designed to assess the antitumor activity of mRNA/LNP formulated fusion proteins compared with that of the FP ref. material. Mice were inoculated on the hind flank with CT26 tumors and when the tumor volume reached ~90 mm^3, treatment began. FP ref. were given at doses of 200 μg through intraperitoneal injection, mRNA/LNPs at 12.5 μg through intravenous injection, and benchmark antibodies at 100 μg through intraperitoneal injection. Treatments were given on days 0, 3, 7, 10, 14, and 17. One cohort of treated animals was assessed for tumor growth and survival over a 30-day period, and another cohort of animals was euthanized on day 8 of the time course, 24 hours after the day 7 dose, to assess therapeutic protein concentrations within the tumor (**A**) and average serum and tumor cytokines for treated animals (**B**). **C,** Individual tumor growth curves are shown for each treatment group. In addition, the average day in which all animals within a treatment group reached tumor burden is quantitated and shown within each graph, and also depicted as a vertical dotted line. The number of animals in each group and any animals that completely rejected the established tumor are also shown within the graphs. For example, the vehicle-treated group reached tumor burden at an average of 13.13 days; 8 animals were in this group and 0/8 rejected the tumor. (*Continued on the following page.*)

We next assessed whether mRNA/LNP formulations of *SIRPα-Fc-CD40L* or *TIGIT-Fc-LIGHT* could delay the growth of established CT26 tumors and extend survival. Once tumors reached an average starting tumor volume of ∼90 mm^3, mice were randomized and treated with either vehicle, anti-CD47, anti-TIGIT, an irrelevant mRNA/LNP negative control, *SIRPα-Fc-CD40L* mRNA/LNP, SIRPα-Fc-CD40L FP ref., *TIGIT-Fc-LIGHT* mRNA/LNP, or TIGIT-Fc-LIGHT FP ref. (**Fig. 4C**). In the control groups, the average time it took for mice to reach tumor burden was approximately 13 to 14 days following the first treatment. SIRPα-Fc-CD40L FP ref. extended the time until reaching tumor burden to 18.80 days and the mRNA/LNP extended this time to 23 days. The TIGIT-Fc-LIGHT FP ref. extended the time until reaching tumor burden to 17.50 days and the mRNA/LNP extended this time to 23 days (**Fig. 4C**). Several of the treated mice completely rejected the established tumors, including with each of the mRNA/LNP groups. The delay in tumor growth induced by the mRNA/LNP and FP ref. constructs also translated into significant survival benefits over the vehicle control (**Fig. 4D**).

Given the antitumor effects and observed changes in both serum and tumor cytokines and chemokines, an analysis of tumor infiltrating lymphocytes was performed. Treg ($CD4^+CD25^+Foxp3^+$) were not elevated in treatment groups, and instead the median percentage of Tregs in the *TIGIT-Fc-LIGHT* mRNA group was 33.9% less than that of the vehicle control. All fusion protein and mRNA treatments increased the infiltration of activated antigen-specific $CD8^+$ T cells into the tumor microenvironment (TME; **Fig. 4E**; Supplementary Fig. S1H). *SIRPα-Fc-CD40L* and *TIGIT-Fc-LIGHT* mRNAs induced the greatest increases in antigen-specific $CD8^+$ T cells into the tumors (AH1 tetramer+), with median values 1.62- and 2.29-fold greater than the vehicle group, respectively.

The efficacy of both SIRPα-Fc-CD40L and TIGIT-Fc-LIGHT were enhanced in combination with tumor targeting antibodies that promote ADCC/ADCP and block checkpoint pathways (10, 11). To further characterize this combination activity with the mRNA-encoding constructs, antitumor activity and the tumor infiltration of antigen-specific $CD8^+$ T cells was evaluated in CT26 tumor bearing animals treated with SIRPα-Fc-CD40L and TIGIT-Fc-LIGHT FP or mRNA/LNP in combination with anti-PDL1 (**Fig. 4F** and **G**). Consistent with previous findings, the combination of all constructs with anti-PDL1, significantly improved tumor growth inhibition compared with anti-PDL1 on its own, with the mRNA/LNP combinations demonstrating improved efficacy relative to the FP combinations (**Fig. 4G**; refs. 10, 11). The mRNA/LNP + anti-PDL1 combination groups also increased intratumoral percentages of $CD8^+CD69^+$ and $CD8^+$AH1-$tetramer^+$ T cells compared with the corresponding monotherapy groups. *SIRPα-Fc-CD40L* mRNA + anti-PDL1 increased $CD8^+CD69^+$ T cells 1.93-fold and $CD8^+$AH1-$tetramer^+$ T cells 2.75-fold greater than anti-PDL1 monotherapy, and *TIGIT-Fc-LIGHT* mRNA + anti-PDL1 increased $CD8^+CD69^+$ T cells 1.72-fold and $CD8^+$AH1-tetramer+ T cells 2.33-fold greater than anti-PDL1 monotherapy (**Fig. 4G**). These results provide confirmation that *SIRPα-Fc-CD40L* and *TIGIT-Fc-LIGHT* mRNA encode functional fusion proteins *in vivo*, which retain the pharmacodynamic and antitumor properties previously described for the recombinant protein versions of these constructs.

Discussion

This study aimed to determine whether lipid encapsulated mRNA could be utilized to deliver complex Fc fusion proteins that require self-association into hexamers through a mixture of covalent and non-covalent interactions, via intravenous infusions. *SIRPα-Fc-CD40L* and *TIGIT-Fc-LIGHT* mRNA/LNP formulations encoded functional fusion protein both *in vitro* and *in vivo*. The kinetics of both *SIRPα-Fc-CD40L* and *TIGIT-Fc-LIGHT* detected concentrations through mRNA/LNP delivery was higher than that achieved with a bolus delivery of recombinant fusion protein and was maintained across at least 96 hours. The progressive increase in expression of CD40L and LIGHT (contained within each fusion protein), closely mirrors the native expression of these and other TNF ligands in the context of a pathogen-induced immune response. In contrast, many TNF receptor agonist therapeutics that are administered by intravenous infusion achieve maximal serum concentrations within a period of minutes and then decay thereafter. Whether these distinct pharmacokinetic profiles contribute to distinct differentiation states of the target cells for each TNF ligand is unknown at this time.

The primary site of *in vivo* protein production using intravenous administered mRNA/LNP is often shown to be the liver, and consistently here, the highest concentrations of both SIRPα-Fc-CD40L and TIGIT-Fc-LIGHT were detected in the serum and liver. Lower—but significant—amounts of both mRNA-encoded proteins were detected in the spleen, lymph node, and within the tumor. This study did not differentiate between protein that was synthesized in a tissue versus proteins accumulated in that tissue via diffusion or active transport from other compartments, however previous work has confirmed the integration of mRNA within these tissues in similar studies (ref. 6 and unpublished data). Regardless of the mechanism, systemic exposure of both SIRPα-Fc-CD40L and TIGIT-Fc-LIGHT was increased when administered as lipid encapsulated mRNA formulations.

The serum concentration of *SIRPα-Fc-CD40L* was high enough to enable the purification and SEC analysis of the *in vivo* expressed protein, and remarkably, the prominent species was shown to exist as a hexamer. When fusion proteins like SIRPα-Fc-CD40L or TIGIT-Fc-LIGHT are produced as recombinant proteins from CHO cells, the final therapeutic exists primarily as a hexamer (10, 11, 22). The observation here that intravenous infusion of mRNA/LNP results in hexameric TNF-ligand containing fusion proteins *in vivo* suggests that the necessary elements for oligomerization are present at the site of *in vivo* translation. In future studies, it would be interesting to extend these observations to other routes of administration, such as intramuscular and subcutaneous (23, 24).

Previously published studies demonstrated antitumor activity for SIRPα-Fc-CD40L and TIGIT-Fc-LIGHT fusion proteins in a range of preclinical models. Those data provided the preclinical

(*Continued.*) **D,** The Kaplan–Maier graph depicts group survival over the time course and the Mantel–Cox test was used to assess group significance. **E,** A cohort of animals was euthanized on day 8, 24 hours after the third dose on day 7. Tumors were excised, dissociated, and the immune infiltrate was assessed by flow cytometry. Truncated violin plots depict the median, first, and third quartiles. **F,** Combination efficacy of FP and mRNA therapeutics was assessed with anti-PDL1 (clone 10F.9G2), which was delivered at doses of 200 μg alone or in the combinations shown on days 0, 3, 7, 10, and 14. Tumor growth inhibition on day 15 of the time course is shown in comparison with the vehicle control group and significance between groups was calculated using unpaired *t* test. **G,** A cohort of treated animals from the combination study was euthanized on day 8, 24 hours after the third dose on day 7. Tumors were excised, dissociated, and the immune infiltrate was assessed by flow cytometry. Cell populations were normalized to those of the anti-PDL1 monotherapy (set at a value of 1) group to visualize the contribution of each combination. *, $P < 0.05$.

basis to advance SIRPα-Fc-CD40L (SL-172154) into clinical trials for patients with platinum resistant ovarian cancer, and also patients with TP53 mutant AML and HR-MDS (NCT05483933 and NCT05275439, respectively), where initial antitumor activity has been observed (10, 11, 25, 26). Despite these data, a potential limitation of this study is that antitumor activity was only demonstrated in a single preclinical mouse tumor model. Using the established CT26 tumor model, mRNA/LNP formulated *SIRPα-Fc-CD40L* and *TIGIT-Fc-LIGHT* compared favorably with the recombinant protein counterparts. Treatment of mice with large established tumors with SIRPα-Fc-CD40L or TIGIT-Fc-LIGHT recombinant protein extended survival in comparison with groups treated with CD47 or TIGIT blocking antibodies. Survival was further improved when the same fusion protein constructs were delivered as mRNA/LNPs, which is likely due to increased exposure within the tumor, and because of prolonged pharmacodynamic effects compared with the recombinant proteins. Delivery of *SIRPα-Fc-CD40L* as mRNA/LNP was associated with increased tumor infiltration of antigen-specific $CD8^+$ T cells, activated APCs, as well as high serum and tumor IL2 levels that were distinct from other groups and persisted over the entire 96-hour time course. Although the increase in IL2 was consistent with *de novo* production, increases in many other serum cytokines occurred within a few hours of treatment, and are likely due to the release of those cytokines and chemokines from preformed granules in circulating immune cells, as has also been shown in human patients with cancer treated with SIRPα-Fc-CD40L (25, 26). In other studies, elevation in chemokines like CCL3 and CCL20 were associated with infiltration of immunosuppressive myeloid and Th17 cells in the TME (27). This study was not focused on the assessment of these cell populations, and future studies could aim to investigate this further.

One of the barriers to delivering biologics using lipid encapsulated mRNAs has been toxicity and immunogenicity associated with the LNP component. Recent advances in LNP and mRNA optimization have reduced these risks, and clinical studies currently underway in children with propionic acidemia (NCT04159103) have demonstrated that mRNA-3957 was well tolerated for over a year of chronic therapy (9). These findings are important as the use of lipid encapsulated nucleic acid technologies continue to broaden into other disease areas that require chronic and sometimes lifelong treatment, for example in various oncology indications or autoimmune disorders. The compelling expression of complex biologics via mRNA/LNP formulations presented here, opens the door to exploring nucleic acid delivery of other therapeutic scaffolds in broader populations of patients, previously thought to be unreachable by an mRNA cargo. Recent studies have shown that lipid encapsulated mRNA can also be used to facilitate *in vivo* production of functional mAbs and T-cell engagers, which do not require oligomerization but instead require assembly of heavy and light chains independently translated from distinct open reading frames (28–31). The speed, cost, and efficiency of mRNA/LNP manufacturing, as well as improved expression, biodistribution, and pharmacodynamics, could result in future approaches where biologics are developed and assessed in parallel with their RNA counterparts, to provide optionality for the optimal targeting of particular receptors or ligands, based on desired PK and PD characteristics that could be uniquely provided by the delivery of a biologic or an mRNA/LNP. The studies herein demonstrate that such approaches may not be limited to individual cytokines, antibodies, or enzymes, but could also apply to complex biologics such as SIRPα-Fc-CD40L and TIGIT-Fc-LIGHT.

Authors' Disclosures

C.W. Shuptrine reports other support from Shattuck Labs outside the submitted work. Y. Chen reports other support from Shattuck Labs outside the submitted work. J. Miriyala reports other support from Shattuck Labs, Inc., outside the submitted work. K. Lenz reports other support from Shattuck Labs, Inc., outside the submitted work. D. Moffett reports other support from Shattuck Labs outside the submitted work. T.T. Nguyen reports other support from Shattuck Labs outside the submitted work. J. Michaux reports other support from Shattuck Labs, Inc., outside the submitted work. K. Campbell reports other support from Shattuck Labs outside the submitted work. C. Smith reports other support from Shattuck Labs outside the submitted work. Y. Rivera-Molina reports other support from Shattuck Labs, Inc., outside the submitted work. N. Murr reports other support from Shattuck Labs, Inc., outside the submitted work. S. Cooper reports other support from Shattuck Labs, Inc., outside the submitted work. V. Makani reports other support from Shattuck Labs, Inc., outside the submitted work. N.P. Oien reports other support from Shattuck Labs, Inc., outside the submitted work. J.T. Zugates reports other support from Shattuck Labs, Inc., outside the submitted work. S. de Silva reports other support from Shattuck Labs, Inc., outside the submitted work. T.H. Schreiber reports personal fees and other support from Shattuck Labs, Inc., outside the submitted work. S. de Picciotto reports employment with Moderna, Inc., and has ownership of Moderna, Inc., stock. G. Fromm reports other support from Shattuck Labs, Inc., outside the submitted work. No disclosures were reported by the other authors.

Authors' Contributions

C.W. Shuptrine: Data curation, formal analysis, supervision, investigation, visualization, methodology. **Y. Chen:** Investigation, methodology. **J. Miriyala:** Investigation, methodology. **K. Lenz:** Investigation, methodology. **D. Moffett:** Writing–review and editing. **T.-A. Nguyen:** Investigation, methodology, writing–review and editing. **J. Michaux:** Investigation, methodology. **K. Campbell:** Investigation. **C. Smith:** Investigation. **M. Morra:** Investigation. **Y. Rivera-Molina:** Investigation. **N. Murr:** Investigation. **S. Cooper:** Investigation. **A. McGuire:** Investigation. **V. Makani:** Investigation. **N. Oien:** Investigation, methodology. **J.T. Zugates:** Investigation, methodology. **S. de Silva:** Writing–review and editing. **T.H. Schreiber:** Conceptualization, formal analysis, supervision, methodology, writing–original draft, writing–review and editing. **S. de Picciotto:** Conceptualization, methodology, writing–original draft, writing–review and editing. **G. Fromm:** Conceptualization, data curation, formal analysis, supervision, visualization, methodology, writing–original draft, writing–review and editing.

Acknowledgments

Funding to complete the work presented in this manuscript was provided by Shattuck Labs, Inc., and Moderna, Inc.

Note

Supplementary data for this article are available at Cancer Research Online (http://cancerres.aacrjournals.org/).

Received September 25, 2023; revised December 22, 2023; accepted February 14, 2024; published first February 21, 2024.

References

1. Kiaie SH, Majidi Zolbanin N, Ahmadi A, Bagherifar R, Valizadeh H, Kashanchi F, et al. Recent advances in mRNA-LNP therapeutics: immunological and pharmacological aspects. J Nanobiotechnology 2022; 20: 276.
2. Zong Y, Lin Y, Wei T, Cheng Q. Lipid nanoparticle (LNP) enables mRNA delivery for cancer therapy. Adv Mater 2023;35:e2303261.
3. August A, Attarwala HZ, Himansu S, Kalidindi S, Lu S, Pajon R, et al. A phase 1 trial of lipid-encapsulated mRNA encoding a monoclonal antibody

with neutralizing activity against Chikungunya virus. Nat Med 2021;27: 2224–33.
4. Jiang L, Park JS, Yin L, Laureano R, Jacquinet E, Yang J, et al. Dual mRNA therapy restores metabolic function in long-term studies in mice with propionic acidemia. Nat Commun 2020;11:5339.
5. de Picciotto S, DeVita N, Hsiao CJ, Honan C, Tse SW, Nguyen M, et al. Selective activation and expansion of regulatory T cells using lipid encapsulated mRNA encoding a long-acting IL-2 mutein. Nat Commun 2022;13:3866.
6. Hewitt SL, Bai A, Bailey D, Ichikawa K, Zielinski J, Karp R, et al. Durable anticancer immunity from intratumoral administration of IL-23, IL-36gamma, and OX40L mRNAs. Sci Transl Med 2019;11:eaat9143.
7. Khattak AC M; Meniawy T; Ansstas G; Medina T; Taylor MH; Kim KB, et al. A personalized cancer vaccine, mRNA-4157, combined with pembrolizumab versus pembrolizumab in patients with resected high-risk melanoma: Efficacy and safety results from the randomized, open-label phase 2 mRNA-4157-P201/ Keynote-942 trial. Am Assoc Cancer Res; 2023.
8. Khattak AW, JS; Menjawy T; Taylor MH; Ansstas G; Kim KB, et al. Distant metastasis-free survival results from the randomized, phase 2 mRNA-4157-P201/KEYNOTE-942 trial. Am Soc Clin Oncol; 2023.
9. Attarwala H, Lumley M, Liang M, Ivaturi V, Senn J. Translational pharmacokinetic/pharmacodynamic model for mRNA-3927, an investigational therapeutic for the treatment of propionic acidemia. Nucleic Acid Ther 2023;33:141–7.
10. de Silva S, Fromm G, Shuptrine CW, Johannes K, Patel A, Yoo KJ, et al. CD40 enhances type I interferon responses downstream of CD47 blockade, bridging innate and adaptive immunity. Cancer Immunol Res 2020;8:230–45.
11. Yoo KJ, Johannes K, Gonzalez LE, Patel A, Shuptrine CW, Opheim Z, et al. LIGHT (TNFSF14) costimulation enhances myeloid cell activation and antitumor immunity in the setting of PD-1/PD-L1 and TIGIT checkpoint blockade. J Immunol 2022;209:510–25.
12. Lakhani NJSD, Richardson DL, Dockery LE, Van Le L, Call J, et al. Phase 1 dose escalation study of SL-172154 (SIRPα-Fc-CD40L) in platinum-resistant ovarian cancer. Am Soc Clin Oncol 2023.
13. Shuptrine CW, Perez VM, Selitsky SR, Schreiber TH, Fromm G. Shining a LIGHT on myeloid cell targeted immunotherapy. Eur J Cancer 2023;187:147–60.
14. Kucka K, Wajant H. Receptor oligomerization and its relevance for signaling by receptors of the tumor necrosis factor receptor superfamily. Front Cell Dev Biol 2020;8:615141.
15. Fromm G, de Silva S, Schreiber TH. Reconciling intrinsic properties of activating TNF receptors by native ligands versus synthetic agonists. Front Immunol 2023; 14:1236332.
16. Croft M, Benedict CA, Ware CF. Clinical targeting of the TNF and TNFR superfamilies. Nat Rev Drug Discov 2013;12:147–68.
17. Nelson J, Sorensen EW, Mintri S, Rabideau AE, Zheng W, Besin G, et al. Impact of mRNA chemistry and manufacturing process on innate immune activation. Sci Adv 2020;6:eaaz6893.
18. Sabnis S, Kumarasinghe ES, Salerno T, Mihai C, Ketova T, Senn JJ, et al. A novel amino lipid series for mRNA delivery: improved endosomal escape and sustained pharmacology and safety in non-human primates. Mol Ther 2018;26: 1509–19.
19. Al Shoyaib A, Archie SR, Karamyan VT. Intraperitoneal route of drug administration: should it be used in experimental animal studies? Pharm Res 2019;37:12.
20. Kunert R, Reinhart D. Advances in recombinant antibody manufacturing. Appl Microbiol Biotechnol 2016;100:3451–61.
21. Johnson MLS, L.L., Hong D; Schoffski P; Galvao V; Rangwala F, et al. Phase 1 dose escalation of an agonist redirected checkpoint (ARC) fusion protein, SL-279252 (PD1-Fc-OX40L), in subjects with advanced solid tumors or lymphomas (NCT03894618). Soc Immunotherapy Cancer; 2022.
22. Fromm G, de Silva S, Johannes K, Patel A, Hornblower JC, Schreiber TH. Agonist redirected checkpoint, PD1-Fc-OX40L, for cancer immunotherapy. J Immunother Cancer 2018;6:149.
23. Munter R, Christensen E, Andresen TL, Larsen JB. Studying how administration route and dose regulates antibody generation against LNPs for mRNA delivery with single-particle resolution. Mol Ther Methods Clin Dev 2023;29:450–9.
24. Pardi N, Tuyishime S, Muramatsu H, Kariko K, Mui BL, Tam YK, et al. Expression kinetics of nucleoside-modified mRNA delivered in lipid nanoparticles to mice by various routes. J Control Release 2015;217:345–51.
25. Lakhani NJSD, Richardson DL, Dockery LE, Van Lee L, Call J, Rangwala F, et al. Phase 1 dose escalation study of SL-172154 (SIRPα-Fc-CD40L) in platinum-resistant ovarian cancer. In Proceedings of the Annual Meeting of the American Society of Hematology; 2023.
26. Daver NSAS, Bixby D, ChaiHo W, Zeidner JF, Maher K, Stevens D, et al. Safety, pharmacodynamic, and anti-tumor activity of SL-172154 as monotherapy and in combination with azacitidine (AZA) in relapsed/refractory (R/Rm) acute myeloid leukemia (AML) and higher-risk myelodysplastic syndromes/neoplasms (HR-MDS) patients (pts). In Proceedings of the Annual Meeting of the American Society of Hematology; 2023.
27. Nagarsheth N, Wicha MS, Zou W. Chemokines in the cancer microenvironment and their relevance in cancer immunotherapy. Nat Rev Immunol 2017;17:559–72.
28. Mukherjee J, Ondeck CA, Tremblay JM, Archer J, Debatis M, Foss A, et al. Intramuscular delivery of formulated RNA encoding six linked nanobodies is highly protective for exposures to three Botulinum neurotoxin serotypes. Sci Rep 2022;12:11664.
29. Hotz C, Wagenaar TR, Gieseke F, Bangari DS, Callahan M, Cao H, et al. Local delivery of mRNA-encoded cytokines promotes antitumor immunity and tumor eradication across multiple preclinical tumor models. Sci Transl Med 2021;13: eabc7804.
30. Liu X, Barrett DM, Jiang S, Fang C, Kalos M, Grupp SA, et al. Improved anti-leukemia activities of adoptively transferred T cells expressing bispecific T-cell engager in mice. Blood Cancer J 2016;6:e430.
31. Wu L, Wang W, Tian J, Qi C, Cai Z, Yan W, et al. Engineered mRNA-expressed bispecific antibody prevent intestinal cancer via lipid nanoparticle delivery. Bioengineered 2021;12:12383–93.